Published by Nigerian Society of Physical Sciences. Hosted by FLAYOO Publishing House LTD

Recent Advances in Natural Sciences

Journal Homepage: https://flayoophl.com/journals/index.php/rans

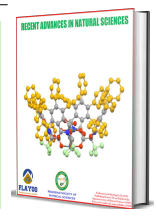

Green synthesis of zinc oxide nanoparticles: A trifecta of antioxidant, antifungal, and catalytic excellence

Abraham Y. Danas[a], Ayomide H. Labulo[a,*], Abdullahi Usman[a], Ibrahim Hassan[a], Augustine D. Terna[b], Festus O. Ogungbemiro[a], David A. Oyinade[c], Ambo A. Idzi[a], Mojisola Owoseni[d], Maryam Isah[e], Rukayat A. Ashonibare[f], Kehinde A.Ojedola[a], Hafsat O. Dahiru[a], Zikhona Tywabi-Ngeva[g], Muhammad A. Said[a], Caroline A. Muaka[h]

[a]*Department of Chemistry, Federal University of Lafia, PMB 146, Lafia, Nasarawa State, Nigeria*
[b]*Department of Chemistry, Federal University of Technology, PMB 1526, Owerri, Imo State, Nigeria*
[c]*Department of Plant Science and Biotechnology, Federal University Oye-Ekiti, Oye-Ekiti, Ekiti State, Nigeria*
[d]*Department of Microbiology, Federal University of Lafia, P.M.B 146, Lafia, Nasarawa State, Nigeria*
[e]*Department of Science Laboratory Technology, Federal University of Lafia, PMB 146, Lafia, Nasarawa State, Nigeria*
[f]*Durable Crops Research Department, Nigerian Stored Products Research Institute, P.M.B. 1489, Ilorin, Kwara State, Nigeria*
[g]*Department of Chemistry, Nelson Mandela University Room: 0003. Floor: Ground. Building: 13. Campus: South, South Africa*
[h]*Department of Psychology, Faculty of Applied Sciences, Daystar University, Kenya*

ARTICLE INFO

Article history:
Received: 25 September 2024
Received in revised form: 04 December 2024
Accepted: 06 December 2024
Available online: 20 December 2024

Keywords: 4-nitrophenol, Antioxidant, Antifungal, Zinc oxide

DOI:10.61298/rans.2024.2.2.127

ABSTRACT

In this study, green synthesis methods were used to fabricate zinc oxide nanoparticles (ZnONPs) using *Newbouldia laevis* leaf extract. Analytical techniques, including Fourier-Transform Infrared Spectroscopy (FTIR), Thermogravimetric Analysis (TGA), Transmission Electron Microscopy (TEM), and UV-Vis spectrophotometer, characterized the green-synthesized ZnONPs. Structural and morphological investigations confirmed successful synthesis. FTIR established functional groups involved in stabilizing and reducing the nanoparticles, while TEM revealed non-spherical particles with well-defined size distribution, crystalline structure, hexagonal morphology, and an average size of 34.8 nm. The ZnONPs demonstrated unique antioxidant properties, with radical scavenging capacity increasing in a concentration-dependent manner. Excellent antifungal activity was observed against *Trichophyton rubrum*, *Aspergillus fumigatus*, and *Candida albicans*, with inhibitory zones ranging from 9 to 18 mm at 100, 200, and 400 mg/mL. Additionally, the ZnONPs showed remarkable photocatalytic reduction of 4-nitrophenol under sunlight. These findings highlight the potential of environmentally friendly ZnONPs for applications in antifungal, antioxidant, and photocatalytic processes.

1. INTRODUCTION

In recent times, nanoscience have become one of the most research areas in chemistry, biology, and engineering [1]. This area of science is multidisciplinary as it involves the manipulation of matter at the atomic state to obtain materials with unique

*Corresponding author: Tel.: +234-806-2295-936
e-mail: ayomide.labulo@science.fulafia.edu.ng (Ayomide H. Labulo)

properties. The synthesis of nanoparticles has evolved over the years from using hazardous chemicals and toxic biodegradable chemicals to a less toxic and environmentally friendly greener approach. ZnO nanoparticles (ZnONPs) have been found to play a vital role in their application in biomedical [2], catalytic [3–5]. This is due to their biocompatibility and unique particle sizes and shapes. Different approaches such as sol-gel [6], co-precipitation [7], thermal decomposition [8], and hydrothermal methods have been explored in the synthesis of ZnONPs. The sol-gel synthetic approach involves the use of toxic chemicals which may be absorbed on the surface of the materials which can largely affect their application in medicine [9]. Green synthesis involving the use of phytochemicals present in plant extract has been explored as a viable alternative. The advantages of plant extract in the synthesis of metal nanoparticles have provided easier routes of synthesizing safe, cost-effective and environmentally friendly nanoparticles. For ZnONPs. these phytochemicals act as the reducing agent replacing the toxic reductant as well as the stabilizing agents [10]. ZnONPs strong antimicrobial properties due to their unique large surface area, facilitating better penetration into the bacteria cells [11]. ZnONPs has been generally found to be safe and less toxic by United State Food and Drug Administration (FDA, 21CFR182.8999) and applicable to the treatment of infectious diseases [12]. Reports have shown the antifungal activities ZnONPs with cell reduction of Candida albican (97.5%) at 100 g/mL exposure [13]. The green synthesis of ZnO nanoparticles with *Allium cepa* (onion) and *Allium sativa* (garlic) and their photocatalytic activities have been studied [14]. Recently, Nandhini *et al*. [15]. reported the green synthesis of ZnONPs using the aqueous leaf extract of *Crataegus oxyacantha* and studied their antioxidant, photocatalytic properties against methylene blue and antifungal properties against *Aspergillus brasiliensis* and *Aspergillus niger*. In comparison to other metal nanoparticles, green synthesized ZnONPs are valuable and effective in clinical and environmental remediation as the phytochemical present in the plant extract usually influences the surface morphology, size and shape of the ZnONPs [15]. Furthermore, extracts from *Moringa oleifera* and *Citrus sinensis* have been widely explored due to their rich phytochemical profiles. For instance, *Moringa oleifera* leaf extracts, abundant in flavonoids and polyphenols, have been used to synthesize ZnONPs with enhanced antimicrobial and antioxidant properties, making them suitable for biomedical applications such as wound healing and drug delivery [16, 17].

Newboudia leavis belongs to the family Bignoniaceae is commonly found in tropical countries in West Africa especially Senegal and some parts in Cameroon and Garbon. It is a scrub that grows between 3-4 meters and a drought tolerant angiosperm [18]. In Nigeria, *Newboudia leavis* is called Akoko in Yoruba, Aduruku in Hausa and Ogirisi in the Igbo speaking part. *Newboudia leavis* bark are commonly used in the treatment of wounds, epilepsy ad convulsion [19]. *Newbouldia laevis* is rich in bioactive compounds which, acts as reducing and capping agents to reduce zinc ions to zinc oxide in the synthesis process. These bioactive compounds also help in stabilizing the nanoparticles, preventing agglomeration and ensuring uniform particles. This makes it a suitable plant for the green synthesis of ZnONPs. *Newbouldia laevis* is widely and readily available, it can be easily grown which also costs less to obtain, thereby making it cost-effective. *Newbouldia laevis* is also non-toxic as reported by Umeyor *et al*. [20], compared to other conventional method for synthesizing nanoparticles, because it does not involve the use of harsh chemicals and high temperatures, making it a sustainable practice. Phytochemicals such as flavonoids, ascorbic acids, carboxylic acid, amino acids, terpenoids, cardiac glycosides and tannins have been reportedly isolated from the leaf of *Newboudia leavis* [21]. Umeyor *et al*. [20] also reported a similar result. These phytochemicals in the *N. laevis* plant extract influence the properties of the synthesized ZnONPs, as they serve as capping, reducing and stabilizing agent of the the synthesis process. To the best of our knowledge *Newboudia leavis* has not been used for the synthesis of ZnO nanoparticles. With an emphasis on the antifungal, antioxidant, and catalytic qualities, this study of the green synthesis of ZnONPs will tackle urgent worldwide issues in environmental management, agriculture, and healthcare [22]. The results may serve as a foundation for further studies aimed at advancing green nanotechnology across a variety of uses [23].

2. MATERIALS

2.1. REAGENTS APPARATUS AND EQUIPMENT

The reagents used in this study are zin sulfate supplied by Sigma Aldrich South Africa (98%). Hydrochloric acid, sodium hydroxide (98%), sodium borohydride and 4-nitrophenol. The equipment used are Erlenmeyer 250 mL beaker, 100 mL standard flasks, 185 μm Whatman filter paper, water bath, analytical scale, aluminum foil, centrifuge, agar plates, autoclave, SEM, UV-vis spectrophotometer, TEM, and FTIR.

2.2. PLANT MATERIAL COLLECTION, IDENTIFICATION AND AUTHENTICATION

Before the preparation, the plant, *Newbouldia laevis* was collected at the area of study, identified, and authenticated at the Department of Botany and Plant Science, Federal University of Lafia.

2.3. PREPARATION OF LEAF EXTRACT

The plant's leaves were removed, thoroughly cleaned with distilled water, and left to dry for at least two weeks at room temperature. Following the drying process, the leaves were chopped into small pieces and cleaned with double distilled water (DDW). In a 250 mL beaker, 5 g of the leaves were cooked for 30 minutes with 100 ml of DDW before being filtered using Whatman number 1 filter paper. For later usage, the filtrate was kept in a refrigerator.

2.4. SYNTHESIS OF ZNO NANOPARTICLES

In the synthesis process, the *Newbouldia laevis* plant extract was used to produce ZnO nanoparticles utilizing the green synthesis approach. Following the previously mentioned preparation of the extract, 30 mL of it was transferred into a beaker and heated gradually. 3 g of zinc nitrate hexahydrate was added to the extract once the temperature had reached 60°C. When the mixture reached a yellowish paste, it was continuously swirled and maintained at 60°C (Figure 1). The obtained slurry solution was then heated for 2 hours in a muffle furnace at 400°C. The obtained

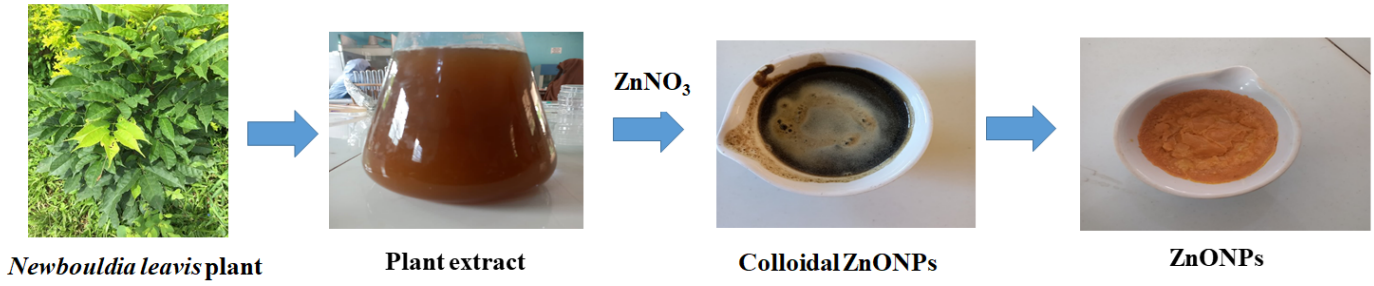

Figure 1. Green synthesis of eco-friendly ZnONPs using the aqueous leave extract of newboudia leavis.

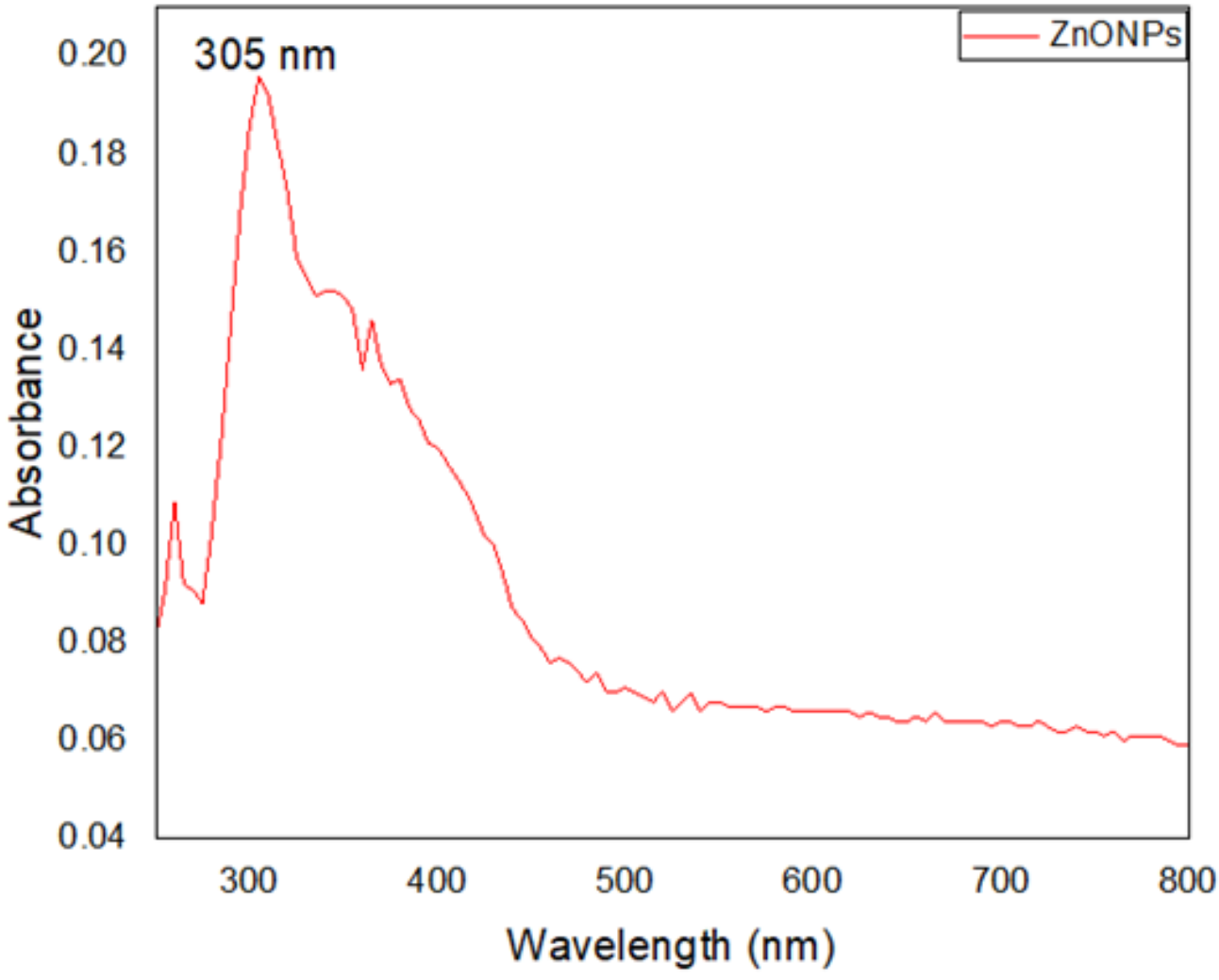

Figure 2. UV-Vis spectrum of synthesized ZnONPs.

yellow pulpy solid was then scrapped into a vial tube and kept at 4°C for further use [24].

2.5. CHARACTERIZATION OF ZNO NANOPARTICLES

The obtained ZnONPs were characterized using both spectroscopic and analytical techniques. The UV-vis spectrophotometer (Jenway 741501) was used to determine the surface plasmon resonance of the synthesized ZnONPs. The surface functionality of the ZnONPs was determined using the Nicolet Summit Fourier-Transform Infra-red (FTIR) spectrophotometer. The surface morphology, shape and size of the ZnONPs was determined using the scanning electron microscopy (SEM) and transmission electron microscopy (TEM, High Angle Annular Dark-Field). The thermal stability was determined using the thermogravimet-

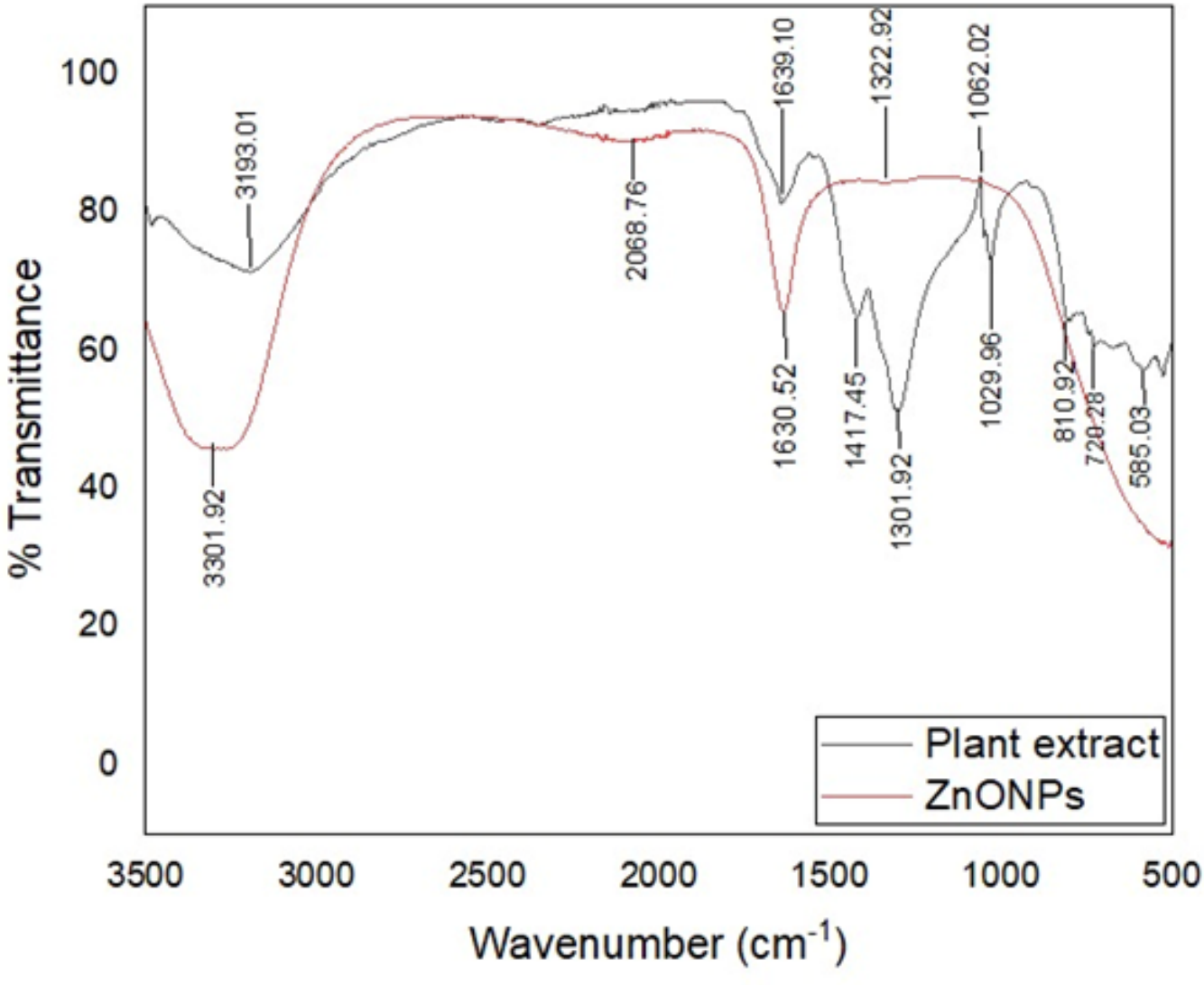

Figure 3. FTIR spectra of ZnONPs.

ric analyser (SDT Q600 V8.3 TGA)

2.6. APPLICATIONS OF SYNTHESIZED ZNO NANOPARTICLES

2.6.1. Determination of Antioxidant Activity

The antioxidant properties of the synthesized ZnONPs was determined using the 2,2-diphenyl-1-picrylhydrazyl (DPPH) method. Using electron transfer, this quick and simple method of screening nanomaterials for antioxidants neutralises free radicals, which cause them to change colour. 1% DPPH was used as the free radical source to assess the nanoparticles' antiradical efficacy. After preparing varying concentrations of ZnONPs (10–100 µg/mL), 1 mL of DPPH and 1 mL of the produced ZnONPs were combined and left in the dark for 20 minutes. After centrifuging the resultant solution for 10 minutes at 14,000 rpm, the UV-vis spectrophotometer was used to examine the clear upper layer that was produced. To get the average findings, the experiment was run three times. The percentage of DPPH scavenging ability was calculated using equation (1).

$$\%\text{DPPH antiradical potency} = \left[\frac{Abs_c - Abs_s}{Abs_c}\right] \times 100, \quad (1)$$

where Abs_c and Abs_c represent the absorption of DPPH in the presence and absence of the sample, respectively.

2.6.2. Determination of Antifungal Activity

Using *Trichophyton rubrum, Aspergillus fumigatus*, and *Candida albicans*, the antifungal activity of synthesised ZnONPs was tested. Potato Dextrose Agar (PDA) was used to cultivate the three isolates. The agar dilution method was used to conduct the antifungal test. The autoclaved PDA medium containing ZnONPs at concentrations of 12.5, 25, 50, 100, 200, and 400 mg/mL as well as an NP-free solution were put into the 9 cm diameter Petri dishes. Following the solidification of the PDA media, the fungi were injected. In the core of each petri dish was a disc (1.4 cm) of mycelial material taken from the periphery of fungal cultures that were 7 days old. The inoculant-filled petri

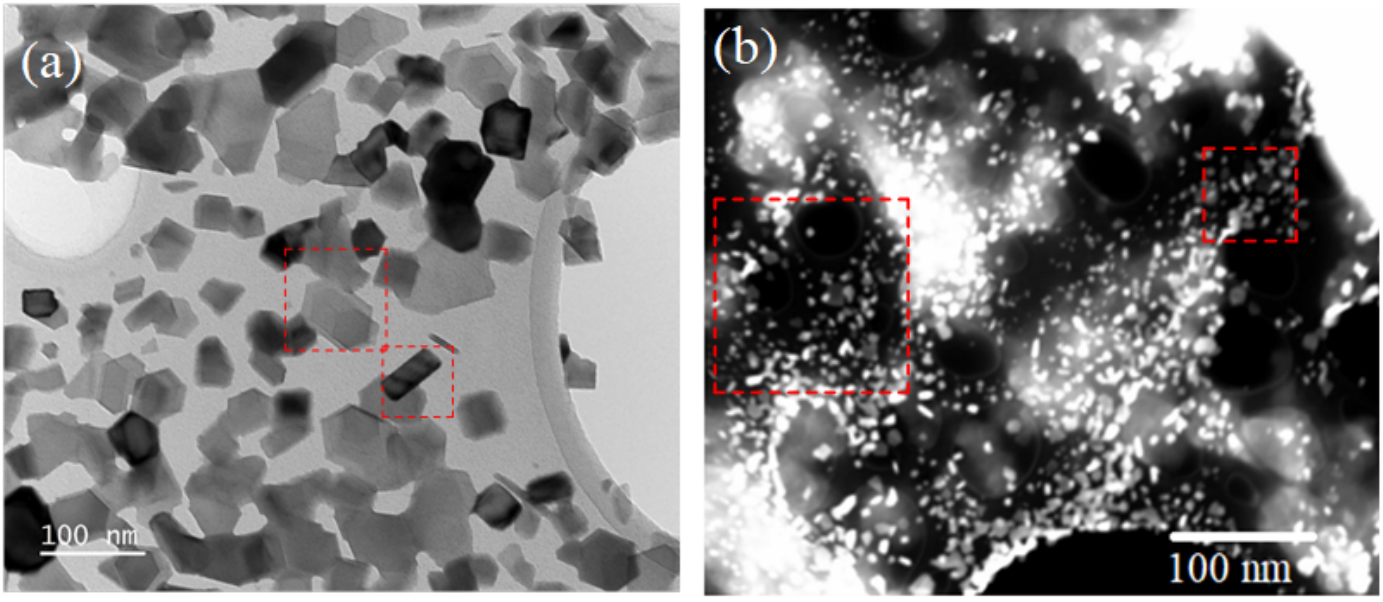

Figure 4. (a) TEM image of ZnONPs (b) HAADF-STEM image of ZnONPs.

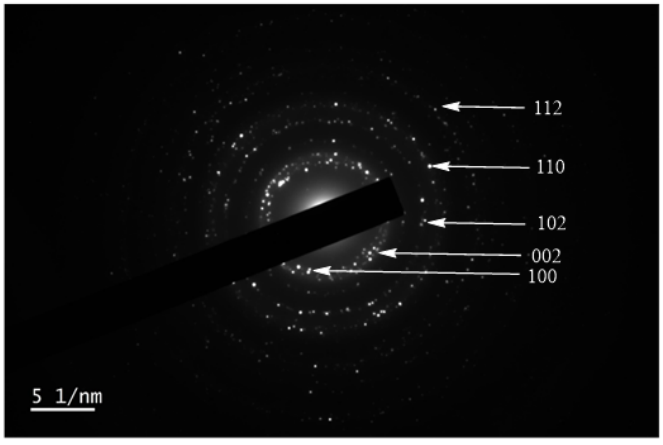

Figure 5. Selected Area Diffraction (SAD) image of ZnONPs.

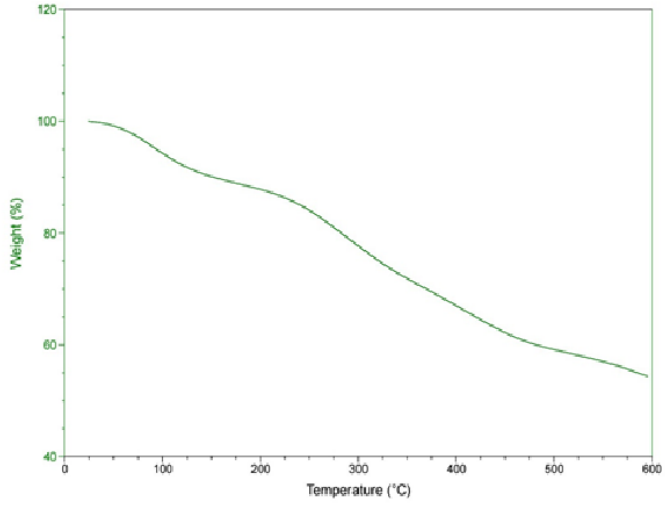

Figure 6. TGA plot of ZnONPs.

dish was incubated at 25 °C. The effectiveness of ZnONP treatment was then assessed at 2, 4, 6, 9, and 12 day intervals [25].

2.6.3. Catalytic Reduction of 4 Nitrophenol by $NaBH_4$

Using UV-Vis spectroscopy, the reduction of 4 nitrophenol was observed at ambient temperature in a quartz cuvette. 3.0 mL of 0.10 mM aqueous solution of 4-NP was combined with with 0.25 mmol of NaBH4 (9.5 mg), and bright yellow solution was formed. The yellow solution was topped off with 1 mg/mL ZnONPs. UV-Vis Spectroscopy was used to track the progress of the reaction at regular intervals within the 250–500 nm scanning range. The yellowish colour of the solution gradually disappears as the reaction continues. Then, equation (2) was used to calculate the 4-NP conversion percentage.

$$\text{Conversion } (\%) = \left(\frac{C_o - C_t}{C_o}\right) \times 100, \qquad (2)$$

where C_t represents the concentration of 4-NP in the solution at time t, while C_o represents the starting concentration of 4-NP in the solution. After the first run, 10 µL of 30 mM 4-NP and 0.25 mmol of $NaBH_4$ (9.5 mg) were added to the reaction system for the second run. For three more runs, this process was repeated [26].

3. RESULTS AND DISCUSSION

3.1. UV-VISIBLE SPECTROSCOPY RESULTS FOR ZNONPS

The synthesis of ZnONPs was identified by monitoring its surface plasmon resonance in the 200–800 nm region using UV-Vis spectroscopy. The UV-visible spectra revealed characteristic absorption peaks that provide light on the properties of the ZnONPs that were synthesised. The absorbance peak at 305 nm, which represents the bandgap energy and the absorption edge

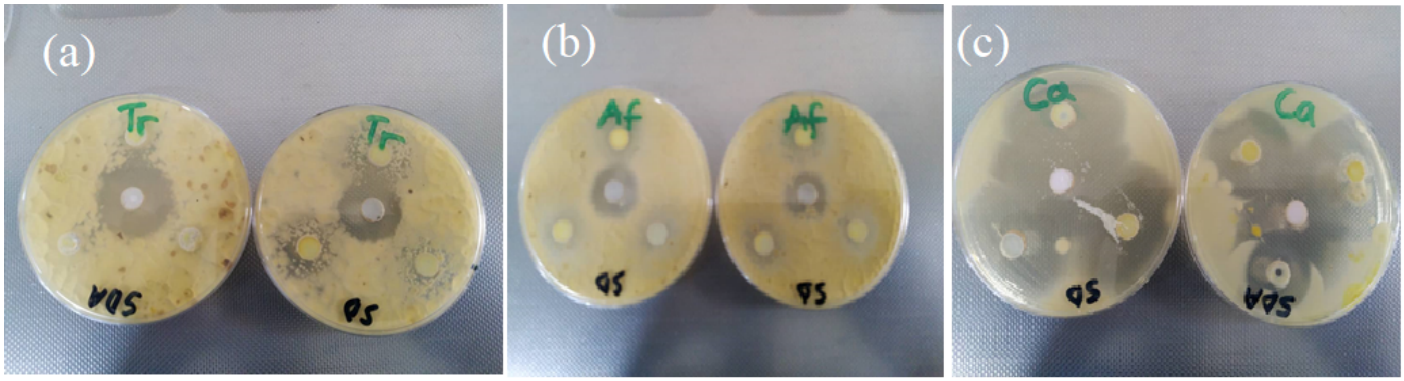

Figure 7. Zone of inhibitions observed by the action of ZnONPs on different fungal isolates. (a) *Trichophyton rubrum* (TR), (b) *Aspergillus fumigatus* (AF), (c) *Candida albicans* (CA).

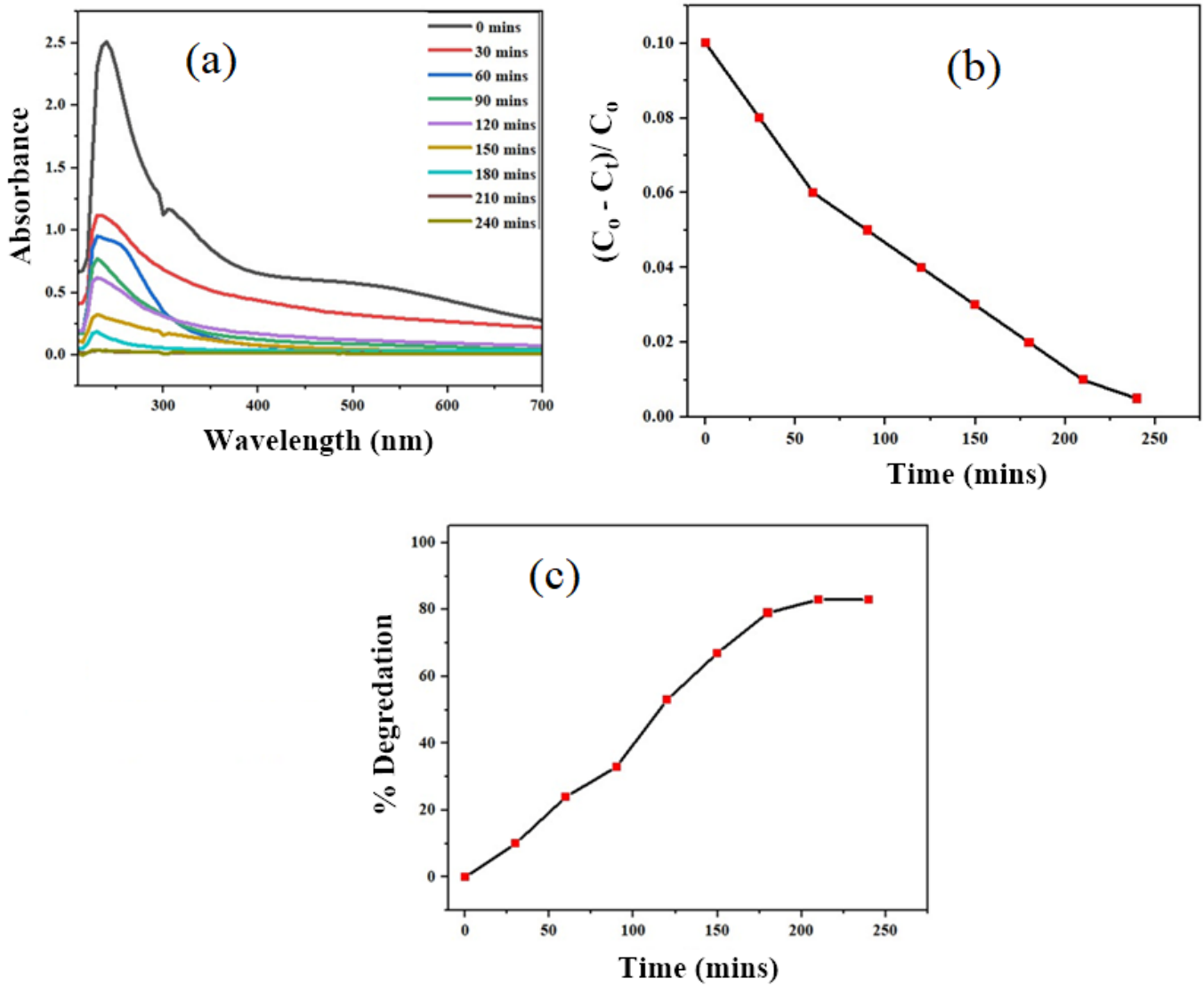

Figure 8. (a) UV plots of the degradation of 4-nitrophenol (b) 4-NPs are photocatalytically degraded with ZnONPs and NaBH4, and (c) How time affects degradation rate.

of ZnONPs, is displayed in Figure 2. The effectiveness of the nanoparticle production process is shown by the intensity of the absorption peak [27].

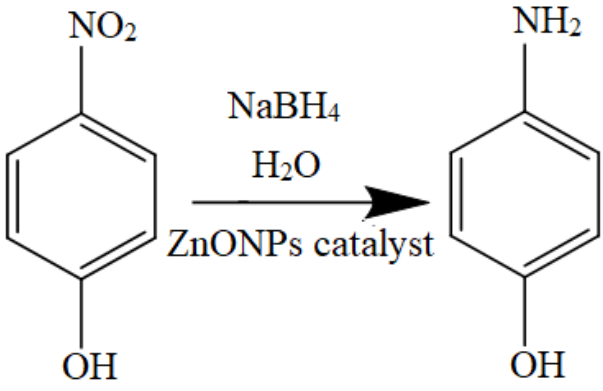

Figure 9. Photocatalytic degradation of 4-NPs using ZnONPs as catalyst.

3.2. FOURIER TRANSFORM INFRARED (FT-IR) SPECTROSCOPY ANALYSIS

The synthesised ZnONPs' surface showed distinctive peaks in the FTIR study that corresponded to unique functional groups. Peaks at 3302, 3193, 2069, 1639, 1631, 1323, 1030, and 585 cm^{-1} were detected by the FTIR analysis (Figure 3). The peaks at 3193 and 3301 cm^{-1} were ascribed to the O-H bond of aromatic compounds (phenol) on the plant extract and synthesized ZnONPs, respectively. The peak at 1631 cm^{-1} was ascribed to the vibrational mode of the nitro compounds [27]. In addition, the peaks at 1323 and 1030 cm^{-1} were assigned to the C-H and C-O stretching mode, respectively. Ezealisiji and co-workers [28] reported similar results. The stabilisation and capping of the synthesised ZnONPs may be attributed to the phenolic in the plant extract. The Zn-O vibration mode is responsible for the absorption band at 585 cm-1, which is consistent with the findings of Jayarambabu and co-workers, suggesting that the ZnONPs were effectively synthesised [27].

3.3. TEM ANALYSIS

The TEM images of the ZnONPs provided detailed insights into the shape and overall structure of the nanoparticles. As depicted in Figure 4a, the ZnONPs produced through the reduction of zinc salt by *Newbouldia laevis* plant extract exhibited a crystalline structure with a hexagonal shape morphology, non-spherical particles with a well-defined size distribution ranging from 22.0 nm to 51.5 nm. It was found that the average nanoparticle size was 34.8 nm similar to the report of Geetha *et al.* [29].

HAADF-STEM analysis: The High Angle Annular Dark Field Scanning Electron Microscopy (HAADF-STEM) image of ZnONPs (Figure 4b) shows that the sample has an irregular form and a considerably scattered size range. The nanoparticles are dispersed randomly throughout the image rather than in a specific order, suggesting no specific clustering or preferential arrangement. This implies that a uniform or well-organized nanostructure was not produced throughout the synthesis process. The red dashed rectangles were inserted to indicate well-dispersed nanoparticulated zinc oxides. Additionally, there is some agglomeration of the nanoparticles in the image, where many particles are joined together. This can be the result of the attraction forces between the particles. Figure 5 shows the selected area diffraction (SAD) pattern, and distribution of the atoms in the crystal lattice of the synthesized ZnONPs. A distinctive ring pattern is observed with the hexagonal wurtzite arrangement with spots representing polycrystalline structures.

Table 1. Antioxidant activity results for ZnONPs.

Concentration (µg/ml)	DPPH Percentage Scavenging (%)	
	ZnO Nanoparticles	Vitamin C (Standard)
10	28.24	5.44
20	29.50	12.76
40	30.33	18.62
60	31.80	25.31
80	32.85	32.64
100	33.26	39.33

3.4. TGA ANALYSIS

Figure 6 shows the thermal stability of the synthesized ZnONPs. The TGA curve shows three main regions. The initial weight loss was from 20-120^{o}C (12%) which is attributed to loss of water. The decomposition of organically bound groups are experienced at the second region between 180-350 °C (25%), while the third region from 350-550 °C is related to the ZnO pure phase formation. No further weight loss was observed beyond 550°C indication of the formation of ZnO nanocrystalline product. This result is similar to the work of Faisal and his co-workers [30].

3.5. ANTIOXIDANT ACTIVITY RESULTS FOR ZNONPS

To determine the antioxidant activity of the ZnONPs, the stability of the DPPH solution was confirmed be leaving it undisturbed for 3 hours with the absorption band remaining at 518 nm with no colour change. Different concentrations of the ZnONPs ranging from 10-100 µg/mL were prepared. These were added to the DPPH followed by colour change from violet to yellow followed by decrease in the absorption peak at 517 nm. This transition could be attributed to substitution of the aromatic ring which increases the molar absorptivity and shift in the absorption band of benzene from a shorter wavelength to a longer one. The observed intensity decrease indicated the free radical scavenging properties of the green synthesized ZnONPs, which is concentration dependent. The scavenging properties increase from 28.24% (10 µg/mL) to 33.26% (100 µg/mL). Although, the vitamin C gave a relatively higher free radical scavenging abilities than the ZnONPs (Table 1).

3.6. ANTIFUNGAL ACTIVITY OF ZNONPS

Using the Agar well diffusion method, the antifungal activity of ZnONPs at varying doses was evaluated against *Trichophyton rubrum*, *Aspergillus fumigatus*, and *Candida albicans* (Table 2). At 100, 200, and 400 mg/mL, the synthesised ZnONPs demonstrated antifungal activity with a zone of inhibition that ranged from 9 to 18 mm. At 400 mg/mL, the three fungal isolates showed the largest zone of inhibition (18 mm). The appearance of inhibitory zones (Figure 7) with zinc oxide nanoparticles

Table 2. *In vitro* **antifungal activity of ZnONPs against fungal isolates.**

	Concentration (mg/mL)/ Diameter of Zone of Inhibition (mm)			Control Amphotericin B (20mg/mL)
	400	200	100	
TR	18	12	10	
TR	14	10	09	
AF	18	13	09	
AF	16	12	09	
				Fluconazole (20 mg/mL)
CA	17	14	12	
CA	18	12	10	

Key: TR = Trichophyton rubrum, AF = Aspergillus fumigatus, CA = Candida albicans

Table 3. *In vitro* **Minimum Inhibitory Concentration (MIC) of ZnO nanoparticles against fungi isolates.**

Organism	Concentration of Extract (µg/mL)						MIC (µg/mL)
	400	200	100	50	25	12.5	
TR	-	- µ	+	+	+	+	200
AF	-	- µ	+	+	+	+	200
CA	-	- µ	+	+	+	+	200

Key: + = Presence of turbidity, - = No turbidity, µ = MIC

Table 4. *In vitro* **Minimum Fungicidal Concentration (MFC) of ZnONPs against fungi isolates.**

Organism	Concentration of Extract (µg/mL)						MFC (µg/mL)
	400	200	100	50	25	12.5	
TR	-	- β	+	+	+	+	200
AF	-	- β	+	+	+	+	200
CA	-	- β	+	+	+	+	200

Key: β = MFC

suggests that pathogens are killed by the nanoparticles' biocidal action mechanism, which involves membrane rupture with a high rate of surface oxygen species formation. The findings of this study are consistent with those of Saravanan and Dalal [31] and Dalal *et al.* [32] who demonstrated in their separate investigations that zinc oxide nanoparticles have an inhibitory impact that is concentration-dependent. ZnONPs have also been shown to exhibit dose-dependent growth inhibitory effects on *Candida albicans*, as reported by Bekele and co-workers [33]. As ZnONP concentration rose, a steady increase in the diameter inhibition zone was observed. The zinc oxide nanoparticles' (ZnONPs) antifungal activity may have resulted from their direct nanoparticle interaction with the fungal cell wall, which caused membrane dysfunction and the generation of reactive oxygen that disrupts intercellular signalling, ultimately causing cell damage and death.

For all examined fungal isolate, the lowest ZnO nanoparticle minimum inhibitory concentration (MIC) (Table 3) and minimum fungicidal concentration (MFC) (Table 4) were 12.5µg/mL. The MIC and MFC measurements revealed that ZnO nanoparticles might be effective inhibitors of fungi isolates. In a similar study, Alshahrani *et al.* [34] and Mendes *et al.* [35], reported 80 µg/mL of ZnONPs as the MIC against *C. albicans*. This report contradicts the result of this present finding. Environmental variables and synthesis techniques may be to blame for this discrepancy, as they have a substantial impact on the nanoparticles' activity.

3.7. CATALYTIC ACTIVITY RESULTS FOR ZNONPS

The degradation of 4-nitrophenol (4-NPs), one of the most prevalent industrial waste pollutants, was used to gauge the catalytic activity of the synthesised ZnONPs. 4-NPs have been found to cause serious damage to human blood, kidneys, and liver [36]. This method evaluates the ability of ZnONPs to catalyze specific reactions. The catalytic tests chosen were designed to investigate the reducing aiding ability of ZnONPs in the reduction of 4-NPs by $NaBH_4$ at room temperature. The results revealed that the reduction did not proceed in the absence of ZnONPs. UV-Vis spectroscopy was employed to track the reaction's development. Without ZnONPs, the maximum absorption of the 245 nm peak does not change. When ZnONPs are added to the solution with 4-NPs and NaBH4, the strong absorption peak at 245 nm gradually loses intensity. After 30 minutes of reaction, the peak diminishes with the gradual disappearance of the yellow colour to colourless after 20 minutes. This indicates the catalytic reduction due to the electron transfer to the 4-NPs acceptor from the BH_4^- (Figure 8a). The effect of ZnNPs as catalysts with $NaBH_4$ is illustrated in Figure 8b. Remarkably, addition of $NaBH_4$ significantly helped promote the reduction in the presence of sunlight (Figure 8b), there was a decrease in the adsorption curve of 4-NPs indicative of the adsorption effect on the catalytic surface. Additionally, aminophenol was obtained via the hydrogen produced from $NaBH_4$. Figure 8c shows a steady degradation rate increase from 0-200 minutes and a constant decrease towards 250 minutes reaction time. This is attributed to the complete degra-

dation of 4-NPs in the presence of the catalyst, this shows similar trajectory as reported by Chishti *et al*. [37], utilizing magnetite silica-core shell for degradation as well as Nasrollahzadeh *et al.*, by utilizing Ag and TiO_2NPs. Figure 9 obstruction of active sites due to the formation of intermediates. ZnONPs catalyst presents a high degradation capacity of 85% within 250 minutes compared to other reports [39, 40].

4. CONCLUSION

In conclusion, ZnONPs were successfully synthesised from the aqueous extract of *Newbouldia leavis* as a reducing agent and stabiliser using a straightforward, economical, environmentally friendly, and greener technique. FTIR, TEM, TGA, and a UV-Vis spectrophotometer were among the analytical methods used to characterise the produced nanoparticles. Green-synthesized ZnONPs show promising antioxidant properties, as well as efficient catalysts for the degradation of 4-NPs. ZnONPs show significant antifungal activity against *Candida albicans, Aspergilus Fumigatus and Trichophyton rubrum.* This greener synthesis approach has competed favourably with conventional and more expensive and toxic synthetic routes and hence a potential catalyst for the treatment of industrial wastewater eluents containing 4-NPs.

ACKNOWLEDGEMENT

This research was funded by the Tertiary Education Trust Fund (TETFund) of the Federal Republic of Nigeria through the Institutional Base Research Fund 2023 (Award Letter Reference Code: FUL/REG/TETFund/002/VOL.V1/047) for the project. The authors acknowledge the Federal University of Lafia and Muhammadu Buhari TETFund Centre of Excellence (MBTCE) for providing the required facilities for this work. Additionally, AHL appreciates Mrs. Rashidat Labulo for proofreading the draft manuscript.

DATA AVAILABILITY

The data supporting the findings of this study are available within the article and its supplementary materials. Raw data, including synthesis parameters, characterization results, and biological activity assays, can be accessed upon request from the corresponding author.

References

[1] S. Bayda, M. Adeel, T. Tuccinardi, M. Cordani & F. Rizzolio, ''The History of Nanoscience and Nanotechnology: From Chemical-Physical Applications to Nanomedicine'', Molecules **25** (2019) 112. https://doi.org/10.3390/molecules25010112.

[2] I. Khan, K. Saeed & I. Khan, ''Nanoparticles: Properties, applications and toxicities'', Arab. J. Chem. **12** (2019) 908. https://doi.org/10.1016/j.arabjc.2017.05.011.

[3] N. Baig, I. Kammakakam & W. Falath, ''Nanomaterials: a review of synthesis methods, properties, recent progress, and challenges'', Mater. Adv. **2** (2021) 1821. https://doi.org/10.1039/D0MA00807A.

[4] D. Li, Q. Lian, T. Du, R. Ma, H. Liu, Q. Liang, Y. Han, G. Mi, O. Peng, G. Zhang, W. Peng, B. Xu, X. Lu, K. Liu, J. Yin, Z. Ren, G. Li & C. Cheng, ''Co-adsorbed self-assembled monolayer enables high-performance perovskite and organic solar cells'', Nat. Commun. **15** (2024) 7605. https://doi.org/10.1038/s41467-024-51760-5.

[5] V. Lotito & T. Zambelli, ''Approaches to self-assembly of colloidal monolayers: A guide for nanotechnologists'', Adv. Colloid Interface Sci. **246** (2017) 217. https://doi.org/10.1016/j.cis.2017.04.003.

[6] S. Hajebi, N. Rabiee, M. Bagherzadeh, S. Ahmadi, M. Rabiee, H. Roghani-Mamaqani, M. Tahriri, L. Tayebi & M. Hamblin, ''Stimulus-responsive polymeric nanogels as smart drug delivery systems'', Acta Biomater. **92** (2019) 1. https://doi.org/10.1016/j.actbio.2019.05.018.

[7] M. Behrens, ''Coprecipitation: An excellent tool for the synthesis of supported metal catalysts – From the understanding of the well known recipes to new materials'', Catal. Today **246** (2015) 46. https://doi.org/10.1016/j.cattod.2014.07.050.

[8] K. Jayaraman, M. V. Kok & I. Gokalp, ''Thermogravimetric and mass spectrometric (TG-MS) analysis and kinetics of coal-biomass blends'', Renew. Energy **101** (2017) 293.https://doi.org/10.1016/j.renene.2016.08.072.

[9] X. Zhang, L. Zhou, X. Tu & F. Hu, ''Hydrothermal synthesis of ZnO Crystals: Diverse morphologies and characterization of the photocatalytic properties'', Polyhedron **246** (2023) 116668. https://doi.org/10.1016/j.poly.2023.116668.

[10] H. Udayagiri, S. S. Sana, L. K. Dogiparthi, R. Vadde, R. S. Varma, J. R. Koduru, G. S. Ghodake, A. R. Somala, V. K. Naidu Boya, S. Kim & R. R. Karri, ''Phytochemical fabrication of ZnO nanoparticles and their antibacterial and anti-biofilm activity'', Sci. Rep. **14** (2024) 19714. https://doi.org/10.1038/s41598-024-69044-9.

[11] A. de Castro Lopes, D. M. de Sousa, G. M. Chaer, F. dos Reis Junior, W. J. Goedert & I. de Carvalho Mendes, ''Interpretation of Microbial Soil Indicators as a Function of Crop Yield and Organic Carbon'', Soil Sci. Soc. Am. J. **77** (2013) 461. https://doi.org/10.2136/sssaj2012.0191.

[12] N. Asif, M. Amir & T. Fatma, ''Recent advances in the synthesis, characterization and biomedical applications of zinc oxide nanoparticles'', Bioprocess Biosyst. Eng. **46** (2023) 1377. https://doi.org/10.1007/s00449-023-02886-1.

[13] A. Lipovsky, Y. Nitzan, A. Gedanken & R. Lubart, ''Antifungal activity of ZnO nanoparticles–the role of ROS mediated cell injury'', Nanotechnology **22** (2011) 105101. https://doi.org/10.1088/0957-4484/22/10/105101.

[14] M. Stan, A. Popa, D. Toloman, A. Dehelean, I. Lung & G. Katona, ''Enhanced photocatalytic degradation properties of zinc oxide nanoparticles synthesized by using plant extracts'', Mater. Sci. Semicond. Process. **39** (2015) 23. https://doi.org/10.1016/j.mssp.2015.04.038.

[15] J. Nandhini, E. Karthikeyan & S. Rajeshkumar, ''Green synthesis of zinc oxide nanoparticles: Eco-friendly advancements for biomedical marvels'', Resour. Chem. Mater. **5** (2024) 1. https://doi.org/10.1016/j.recm.2024.05.001.

[16] H. Perumalsamy, S. R. Balusamy, J. Sukweenadhi, S. Nag, D. MubarakAli, M. El-Agamy Farh, H. Vijay & S. Rahimi, ''A comprehensive review on Moringa oleifera nanoparticles: importance of polyphenols in nanoparticle synthesis, nanoparticle efficacy and their applications'', J. Nanobiotechnology, **22** (2024) 71. https://doi.org/10.1186/s12951-024-02332-8.

[17] Y. Gao, D. Xu, D. Ren, K. Zeng & X. Wu, ''Green synthesis of zinc oxide nanoparticles using Citrus sinensis peel extract and application to strawberry preservation: A comparison study'', LWT **126** (2020) 109297. https://doi.org/10.1016/j.lwt.2020.109297.

[18] I. S. Dassekpo, E. G. Achigan-Dako, B. Tenté, C. S. Houssou & A. Ahanchédé, ''Valuation of Newbouldia laevis and its endogenous conservation in Benin (West Africa)'', J. Herb. Med. **23** (2020) 100388. https://doi.org/10.1016/j.hermed.2020.100388.

[19] J. B. Habu & B. O. Ibeh, ''In vitro antioxidant capacity and free radical scavenging evaluation of active metabolite constituents of Newbouldia laevis ethanolic leaf extract'', Biol. Res. **48** (2015) 16. https://doi.org/10.1186/s40659-015-0007-x.

[20] C. Umeyor, E. Anaka, F. Kenechukwu, C. Agbo & A. Attama, ''Development, in vitro and in vivo evaluations of novel lipid drug delivery system of Newbouldia laevis (P. Beauv.)'', Nanobiomedicine **3** (2016) 1. https://doi.org/10.1177/1849543516673445.

[21] T. G. Atere, O. A. Akinloye, R. N. Ugbaja, D. A. Ojo & G. Dealtry, ''In vitro antioxidant capacity and free radical scavenging evaluation of standardized extract of Costus afer leaf'', Food Sci. Hum. Wellness **7** (2018) 266. https://doi.org/10.1016/j.fshw.2018.09.004.

[22] D. C. Bouttier-Figueroa, M. Cortez-Valadez, M. Flores-Acosta & R. E. Robles-Zepeda, ''Green synthesis of zinc oxide nanoparticles using plant extracts and their antimicrobial activity'', Bionanoscience **14** (2024) 3385. https://doi.org/10.1007/s12668-024-01471-4.

[23] D. Sarpong, D. Boakye, G. Ofosu & D. Botchie, ''The three pointers of research and development (R&D) for growth-boosting sustainable innovation system'', Technovation **122** (2023) 102581. https://doi.org/10.1016/j.technovation.2022.102581.

[24] Y. A. Selim, M. A. Azb, I. Ragab & M. H. M. A. El-azim, ''Green syn-

thesis of zinc oxide nanoparticles using aqueous extract of deverra tortuosa and their cytotoxic activities'', Sci. Rep. (2022) 1. https://doi.org/10.1038/s41598-020-60541-1.

[25] L. He, Y. Liu, A. Mustapha & M. Lin, ''Antifungal activity of zinc oxide nanoparticles against Botrytis cinerea and Penicillium expansum'', Microbiol. Res. **166** (2011) 207. https://doi.org/10.1016/j.micres.2010.03.003.

[26] G. Wu, X. Liang, L. Zhang, Z. Tang, M. Al-Mamun, H. Zhao & X. Su, ''Fabrication of highly stable metal oxide hollow nanospheres and their catalytic activity toward 4 - nitrophenol reduction'', ACS Appl. Mater. Interfaces **9** (2017) 18207. https://doi.org/10.1021/acsami.7b03120.

[27] N. Jayarambabu, B. S. Kumari, K. V. Rao & Y. T. Prabhu, ''Germination and growth characteristics of mungbean seeds (vigna radiata l.) affected by synthesized zinc oxide nanoparticles'', Int. J. Curr. Eng. Technol. **4** (2014) 3412. https://inpressco.com/wp-content/uploads/2014/09/Paper593411-3416.pdf.

[28] K. M. Ezealisiji, S.-N. Xavier, B. Maduelosi & N. Nwachukwu, ''Green synthesis of zinc oxide nanoparticles using Solanum torvum (L) leaf extract and evaluation of the toxicological profile of the ZnO nanoparticles – hydrogel composite in Wistar albino rats'', Int. Nano Lett. **9** (2019) 99. https://doi.org/10.1007/s40089-018-0263-1.

[29] M. S. Geetha, H. Nagabhushana & H. N. Shivananjaiah, ''Green mediated synthesis and characterization of ZnO nanoparticles using Euphorbia Jatropa latex as reducing agent'', J. Sci. Adv. Mater. Devices **1** (2016) 301. https://doi.org/10.1016/j.jsamd.2016.06.015.

[30] S. Faisal, H. Jan, S.Ali Shah, S. Shah, A. Khan, M. T. Akbar, M. Rizwan, F.Jan, W. N. Akhtar, A. Khattak & S. Syed, ''Green Synthesis of Zinc Oxide (ZnO) Nanoparticles Using Aqueous Fruit Extracts of Myristica fragrans : Their Characterizations and Biological and Environmental Applications'', Am. Chem. Soc. Omega **6** (2021) 9709. https://doi.org/10.1021/acsomega.1c00310.

[31] S. Saravanan & D. R. S. Dubey, ''Synthesis of SiO2 Nanoparticles by Sol-Gel Method and Their Optical and Structural Properties'', Rom. J. Inf. Sci. Technol. **23** (2020) 105. https://www.romjist.ro/full-texts/paper641.pdf.

[32] M. Dalal, A. Das, D. Das, R. S. Ningthoujam & P. K. Chakrabarti, ''Studies of magnetic, Mössbauer spectroscopy, microwave absorption and hyperthermia behavior of Ni-Zn-Co-ferrite nanoparticles encapsulated in multi-walled carbon nanotubes'', J. Magn. Magn. Mater. **460** (2018) 12. https://doi.org/10.1016/J.JMMM.2018.03.048.

[33] S. G. Bekele, D. D. Ganta & M. Endashaw, ''Green synthesis and characterization of zinc oxide nanoparticles using Monoon longifolium leave extract for biological applications'', Discov. Chem. **1** (2024) 5. https://doi.org/10.1007/s44371-024-00007-9.

[34] S. M. Alshahrani, E.-S. Khafagy, Y. Riadi, A. Al Saqr, M. M. Alfadhel & W. A. H. Hegazy, ''Amphotericin B-PEG Conjugates of ZnO Nanoparticles: Enhancement Antifungal Activity with Minimal Toxicity.'', Pharmaceutics **14** (2022) 1646. https://doi.org/10.3390/pharmaceutics14081646.

[35] C. R. Mendes, G. Dilarri, C. F. Forsan, V. de Moraes Ruy Sapata, P. R. M. Lopes, P. Bueno de Moraes, R. N. Montagnolli, H. Ferreira & Ederio Dino Bidoia , ''Antibacterial action and target mechanisms of zinc oxide nanoparticles against bacterial pathogens'', Sci. Rep. **12** (2022) 2658. https://doi.org/10.1038/s41598-022-06657-y.

[36] A. Garjani, ''Pharmaceutical sciences'', Pharm. Sci. **22** (2016) 1. https://doi.org/10.15171/PS.2016.01.

[37] A. N. Chishti, L. Ni, F. Guo, X. Lin, Y. Liu, H. Wu, M. Chen, G. Wang Diao, ''Magnetite-Silica core-shell nanocomposites decorated with silver nanoparticles for enhanced catalytic reduction of 4-nitrophenol and degradation of methylene blue dye in the water'', J. Environ. Chem. Eng. **9** (2021) 104948. https://doi.org/10.1016/j.jece.2020.104948.

[38] M. Nasrollahzadeh, M. Atarod, B. Jaleh & M. Gandomirouzbahani, ''In situ green synthesis of Ag nanoparticles on graphene oxide/TiO2 nanocomposite and their catalytic activity for the reduction of 4-nitrophenol, congo red and methylene blue'', Ceram. Int. **42** (2016) 8587. https://doi.org/10.1016/j.ceramint.2016.02.088.

[39] J. Chen, Z. Wu, J. Zheng, Y. Shi, L. Xie, F. Yang, Y. Wang, Z. Zhang, ''Novel solid-state hydrolysis kinetics of NaBH4 for stable and high-capacity on-line hydrogen production'', Chem. Eng. J. **486** (2024) 150062. https://doi.org/10.1016/j.cej.2024.150062.

[40] G. Zhou, Z. He & X. Dong, ''Role of Metal Oxides in Cu-Based Catalysts with NaBH4 Reduction for the Synthesis of Methanol from CO2/H2'', Catal. Letters **151** (2021) 1091. https://doi.org/10.1007/s10562-020-03379-6.